CHALMERS
UNIVERSITY OF TECHNOLOGY

Design and Fabrication of a High Gain 60-GHz Cavity-backed Slot Antenna Array fed by Inverted Microstrip Gap Waveguide

Citation for the original published paper (version of record):
Liu, J., Vosoogh, A., Uz Zaman, A. et al (2017). Design and Fabrication of a High Gain 60-GHz Cavity-backed Slot Antenna Array fed by Inverted
Microstrip Gap Waveguide. IEEE Transactions on Antennas and Propagation, 65(4): 2117-2122.
http://dx.doi.org/10.1109/TAP.2017.2670509

Design and Fabrication of a High Gain 60-GHz Cavity-backed Slot Antenna Array fed by Inverted Microstrip Gap Waveguide

Jinlin Liu, Abbas Vosoogh, Ashraf Uz Zaman, and Jian Yang

Abstract

This paper deals with the design of a 16×16 slot array antenna fed by inverted microstrip gap waveguide (IMGW). The whole structure designed in this work consists of radiating slots, a groove gap cavity layer, a distribution feeding network and a transition from standard WR-15 waveguide to the IMGW. Firstly, a 2×2 cavity-backed slot sub-array is designed with periodic boundary condition to achieve good performances of radiation pattern and directivity. Then a complete IMGW feeding network with a transition from WR-15 rectangular waveguide to the IMGW has been realized to excite the radiating slots. The complete antenna array is designed at 60-GHz frequency band and fabricated using Electrical Discharging Machining (EDM) technology. The measurements show that the antenna has a 16.95% bandwidth covering 54-64 GHz frequency range. The measured gain of the antenna is more than 28 dBi with the efficiency higher than 40% covering 54-64 GHz frequency range.

1 Introduction

Recently, considerable attention has been paid to 60-GHz frequency band. Communications distances at the frequency band are limited by a high attenuation caused by the atmosphere absorption. Thereby, high gain and wide bandwidth characteristics are required for the antennas. Among all antenna types a slot array is suitable for the realization at 60-GHz band. The target of this work is to design a planar slot array based on inverted microstrip gap waveguide (IMGW) technology, which is recently introduced as a suitable guiding structure for millimeter wave (mmW) systems. The conception of the IMGW can be modeled for theoretical analysis by two parallel plates, a top Perfect Electric Conductor (PEC) layer and a bottom Perfect Magnetic Conductor (PMC) layer, with a metallic strip placed in the bottom PMC layer. This structure stops all modes propagating in all directions except for a quasi-TEM mode along the strip over a specific frequency band (stopband) when the gap between PEC and PMC plates is smaller than quarter wavelength at an operation frequency [1]. Besides IMGW there are also other three different versions of

gap waveguide — groove, ridge [2] and microstrip-ridge gap waveguides [3]. Many research works have been published on the gap waveguide technology in fields of antennas [4-8], microwave filters [9-10] and the packaging for microwave circuits [11-12]. In this paper, we systematically present a 16×16 slot antenna array designed with IMGW corporate feeding networks. In section II, we elaborate the design of a 2×2 sub-array at 60-GHz. The corporate feed networks based on IMGW technology is explained in section III. Section IV is devoted to the simulated and measured results of whole antenna structure. Finally, summary and conclusions are presented in section V.

2 Design for 2×2 Sub-array

The gap waveguide technology uses a parallel-plate stopband over a specific frequency range. The dimensions of the pins of the bed of nails at the bottom should be chosen correctly to achieve a stopband which covers as much as 60-GHz frequency band [13]. We carried out a numerical parametric analysis in this work of the IMGW whose structure is illustrated in Fig. 1(a). The corresponding dispersion diagram of the

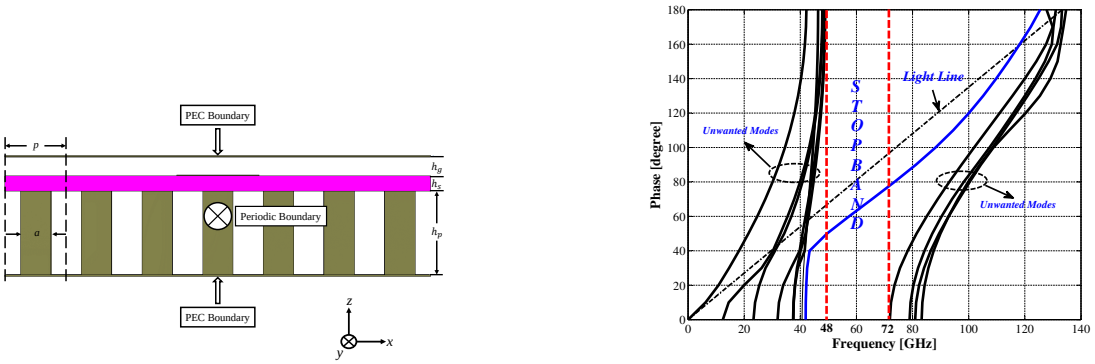

(a) (b)

Figure 1: (a) 2-dimensional view of the unit cell. (b) Dispersion diagram of the unit cell utilized in (a) [$h_s = 0.2$ mm, $h_g = 0.25$ mm, $h_p = 1.2$ mm, $a = 0.4$ mm and $p = 0.8$ mm]. The blue line indicates the quasi-TEM mode.

structure is shown in Fig. 1(b), which indicates that only the quasi-TEM mode can propagate along the inverted microstrip line but the other modes are stopped in the frequency band from 48 to 72 GHz. The substrate material is Rogers RO4003 with relative permittivity $\varepsilon_r = 3.55$, loss tangent $tan\delta = 0.0027$ (specified at 10 GHz by Rogers) and thickness $h_s = 0.2$ mm. The motivations to select RO4003 are that it has a lower loss value than traditional PCB substrate FR4 and is mechanically rigid enough for our case.

The configuration of a 2×2-element sub-array is firstly designed using periodic

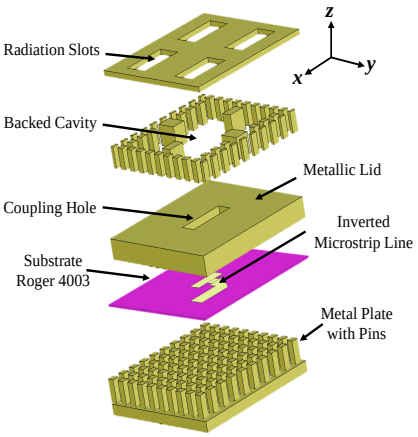

Figure 2: Detailed 3-D view of 2 × 2 slots sub-array.

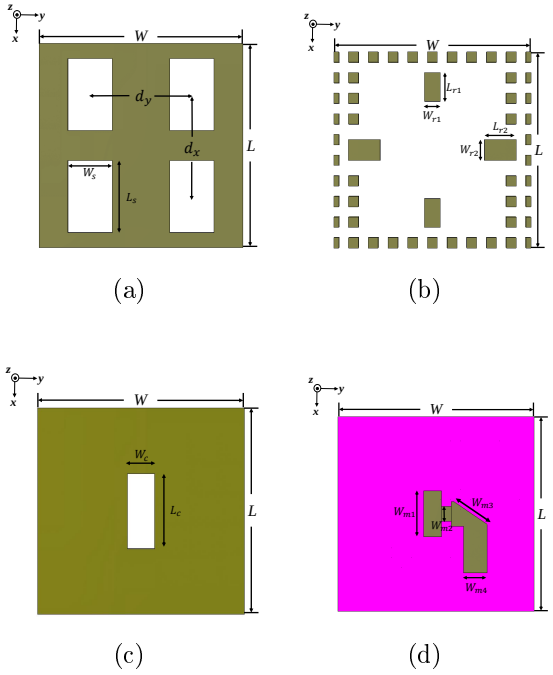

Figure 3: Geometrical parameters of a 2×2 slots array. (a) Top radiation slots layer. (b) Backed cavity layer. (c) Coupling hole layer. (d) Feed distribution networks layer.

boundary condition in CST Microwave Studio in order to evaluate the radiation pattern and directivity of the whole array antenna, as shown in Fig. 2. It consists of a radiating slot layer, a cavity layer, a PCB microstrip layer and a bed of nails at the bottom. Instead of a normal hollow rectangular waveguide cavity, we have utilized a groove gap cavity here for easy manufacture. The groove gap cavity is partitioned

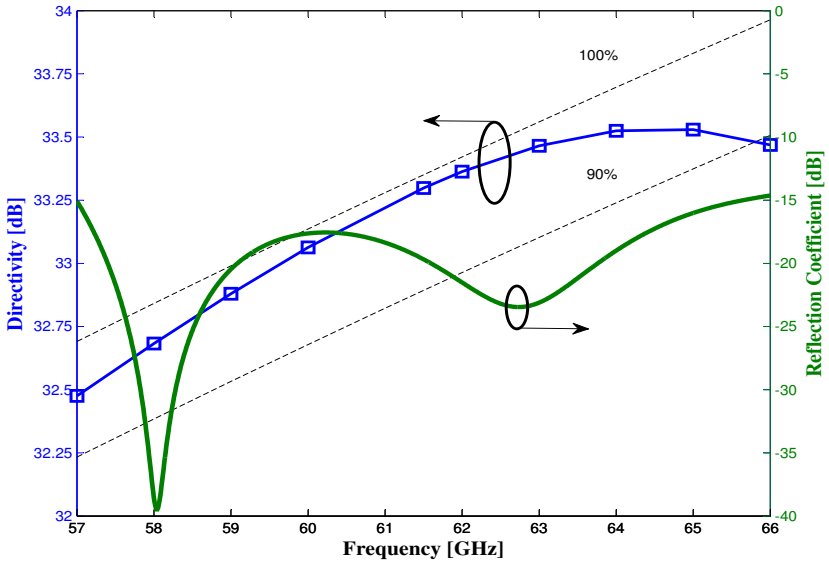

Figure 4: The simulated directivity and reflection coefficient of the 2×2 sub-array.

into four spaces by two sets of metallic blocks extending in the x and y directions. The PCB microstrip layer feeds the four spaces of groove gap cavity with identical phase and amplitude by the center coupling hole in the cavity layer.

The slots are uniformly spaced in both x and y directions with a spacing smaller than one wavelength in order to avoid grating lobes in a large broadside array. The highest frequency for this work is 66 GHz and the corresponding wavelength λ is about 4.5 mm. Therefore, the slot space d_s in this work is chosen as 4 mm. On the other hand, the value W and L should be integer times of the pins period, namely $W = Mp$ and $L = Np$. Given the above-mentioned considerations, we select $W = L = 10p = 8$ mm. The detailed geometrical demonstrations of the antenna sub-array are shown in TABLE I. In Fig. 4 the green line shows the reflection coefficient of the sub-array and an 14.5% impedance bandwidth (over 57-65.7 GHz) with the input reflection coefficient below -15 dB is achieved. The blue line with square mark in the figure illustrates the simulated directivity of the 16×16 slot array in infinite array environment. The simulated antenna efficiency is higher than 90% from 57 to 65.9 GHz.

3 Design of Feeding Distribution Network

Compared with the groove and the ridge gap waveguide structures [2], the feeding distribution network based on the IMGW technology has some obvious advantages.

Table 1: Dimensional Parameters of 2×2 unit cell referring to Fig. 3

Substrate Material	Rogers 4003 (ε^*=3.55)
W	8 mm
L	8 mm
d_x	4 mm
d_y	4 mm
W_s	1.748 mm
L_s	2.832 mm
W_{r1}	0.637 mm
L_{r1}	1.111 mm
W_{r2}	0.811 mm
L_{r2}	1.277 mm
W_c	1.071 mm
L_c	2.742 mm
W_{m1}	1.883 mm
W_{m2}	0.607 mm
W_{m3}	1.642 mm
W_{m4}	1.05 mm

First of all, it has a uniform bed of nails while the others do not. This uniform pin structure makes the fabrication much easier and cheaper. Secondly, fabrication of microstrip circuitry on PCB by etching is accurate and very low cost. Thirdly, theories and design principles of traditional inverted microstrip technique are matured so we can directly utilize them with little modifications. For these reasons, the IMGW structure is attractive in feeding networks for slot antenna arrays at mmW frequencies.

Despite its advantages, there are still challenges in design of IMGW feeding distribution networks. In [5] a planar horn array fed by an IMGW feeding network has been already expounded. Since the metallic pin surface can be modeled approximately by PMC boundary condition, the distribution network in [5] was designed with an ideal PMC condition instead of the real metallic pin structure located at the bottom plate. Differently, the corporate-feed network in the present work is designed by applying the real pin structure in the design process because there exists evanescent electromagnetic fields in the substrate and the pin structure, which though small affects the propagation of the quasi-TEM mode and losses. Therefore, assuming an ideal PMC condition to replace the metallic pins structure may give rise to a significant error in the design of feeding distribution networks. As shown in Fig. 5(a) *left*, a simple straight IMGW structure is firstly modeled in CST Microwave Studio with PMC boundary condition at the bottom plate. Then we also modeled the periodic

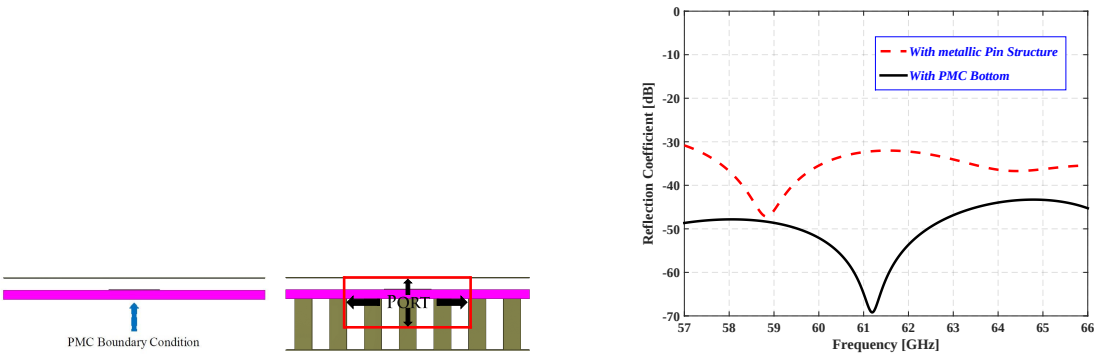

(a) (b)

Figure 5: Discrepancy between the ideal model and the realistic model. (a) The left figure illustrates a covered microstrip line with PMC boundary condition at the bottom. In the right one the PMC boundary condition is replaced by metallic pins. (b) The black solid line shows the simulated reflection coefficient with the PMC boundary condition at the bottom. The red dash line indicates the reflection coefficient with the metallic pins at the bottom in the first structure.

pins structure in Fig. 5(a) *right* in order to see the effect of the real pin structure. The corresponding results as shown in Fig. 5(b) for both models verified the existing error in [5]. Therefore, we utilize the real pin structure in the present design of the whole feeding network to obtain accurate performances.

The IMGW feeding element for the 2×2 sub-array is present in Section II. T-junction power dividers with matching circuits are used in our feeding network. Essentially a T-junction power divider is a simple three-port network that can be utilized for power division or combining. Thereby, the T-junction is a central component in the distribution network for feeding the antenna array. In this work we designed a T-junction power divider with metallic pins at the bottom in CST Microwave Studio, as shown in Fig. 6. In order to obtain correct transition performance an optimized numerical port [14] has been utilized during the entire design procedure. The T-junction then has been optimized for the minimum reflection coefficient and the corresponding S-parameters are shown in Fig. 7, in which the reflection coefficient S_{11} is below -30 dB from 57 to 66 GHz. Also, for the determination of the loss caused by the substrate, aluminum pins and copper strip we have twice simulated the T-junction. The transmission coefficients of the lossy case are around 0.2 dB lower than these values of the lossless case and the leakage loss is a negligible value of 0.02 dB.

The aim of the matching networks is to eliminate the reflection effect on the distribution networks. In this work we apply a classical second order binomial impedance transformer for impedance matching. All characteristic impedances and load impedances have been obtained from optimized numerical ports introduced in [14]. Here we should notice that part 1 of matching microstrip in Fig. 8 has been

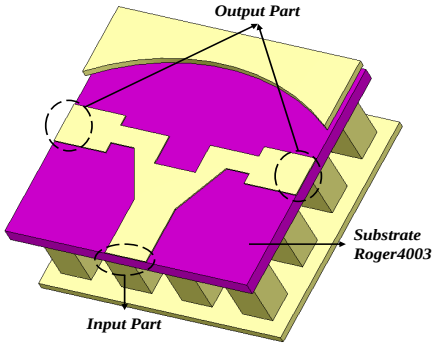

Figure 6: 3-dimensional view for the T-junction with metallic pins at the bottom.

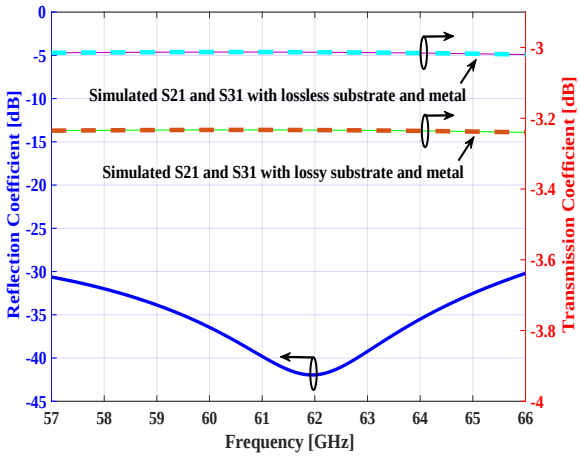

Figure 7: Simulated S-parameters of single T-junction in Fig. 6 for both lossy and lossless cases.

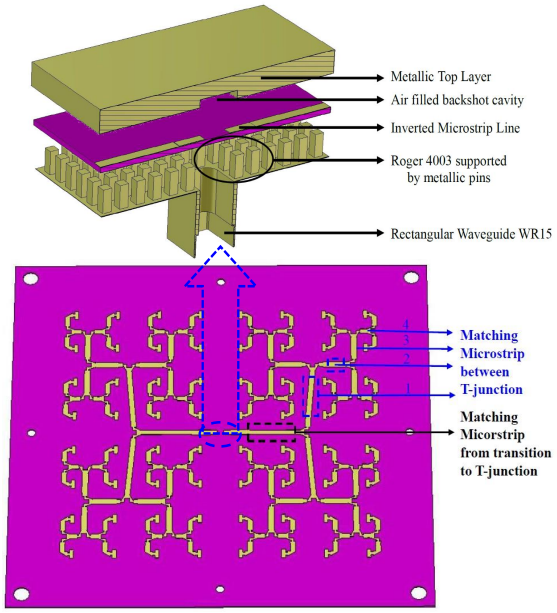

Figure 8: Illustration for the whole feeding networks including T-junction power dividers, matching microstrips and a transition power divider from WR-15 to the IMGW structure.

designed in a shape of parallelogram in order to remove its mutual coupling to the nearest coupling holes.

The input port of the array antenna is required to be WR-15 rectangular waveguide. A novel power divider transition in [15] was applied in this work. The simulated reflection coefficient of the transition is below -20 dB and the phases of the output ports have 180 degree difference. The complete corporate-feed network consists of two 32-way power dividers connected to the transition of WR-15 in the center. Due to the out-of-phase output of the transition, the two 32-way power dividers are in a mirror geometry in order to have the same phase excitations for all slots. The final designed structure of the feeding distribution network is shown in Fig. 8. Finally, the whole distribution network is optimized by genetic algorithm in CST Microwave Studio.

4 Simulated and experimental Results

The numerical model and the final manufactured prototype of the 16×16 slot array antenna are shown in Fig. 9. The metallic parts of the antenna are fabricated by Electrical Discharging Machining (EDM) Technology, where the prototype is etched by recurring electric discharges between the workpiece and electrodes. The designed array aperture dimension is $64 \times 64\ mm^2$.

The simulated and measured input reflection coefficients of the antenna are shown

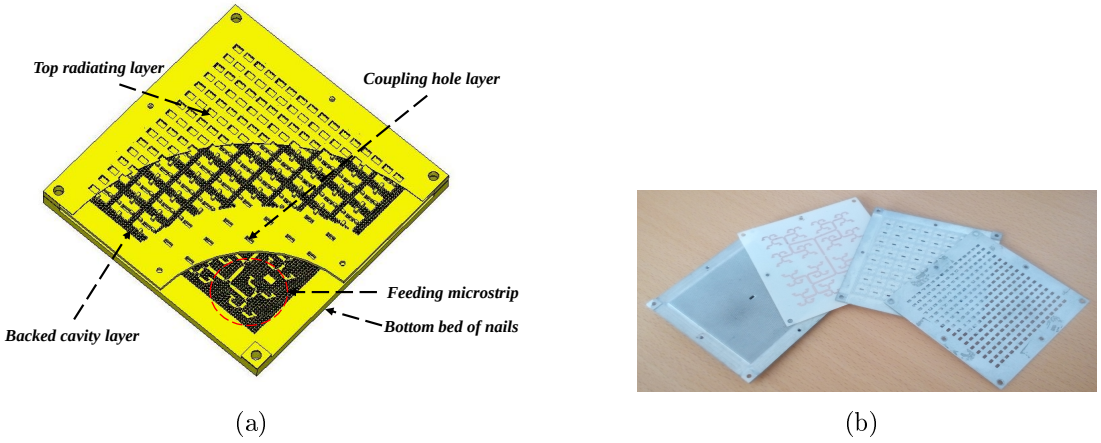

(a) (b)

Figure 9: (a) Numerical model of the proposed array antenna in CST Microswave studio . In order to observe the microstrip and waveguide open details the substrate is hidden. (b) Photogragh of the proposed 16×16 array antenna fabricated by EDM technology.

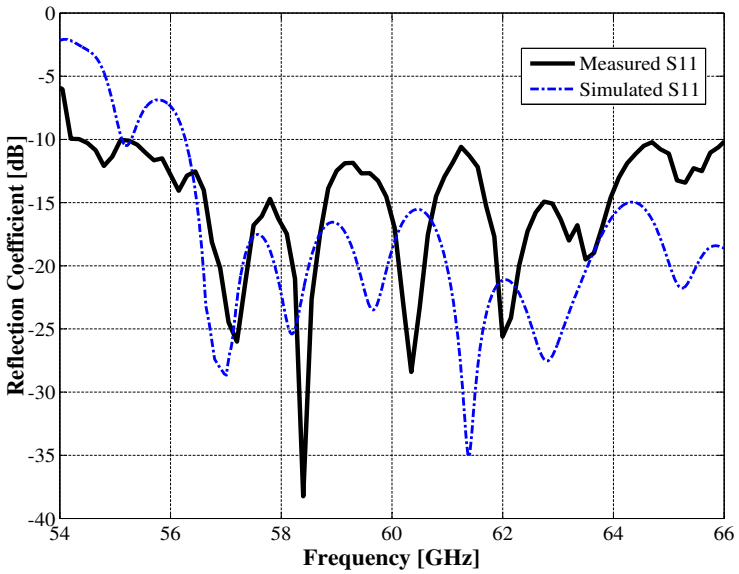

Figure 10: Comparison of simulated and measured reflection coefficient of the proposed 16×16 slot array antenna.

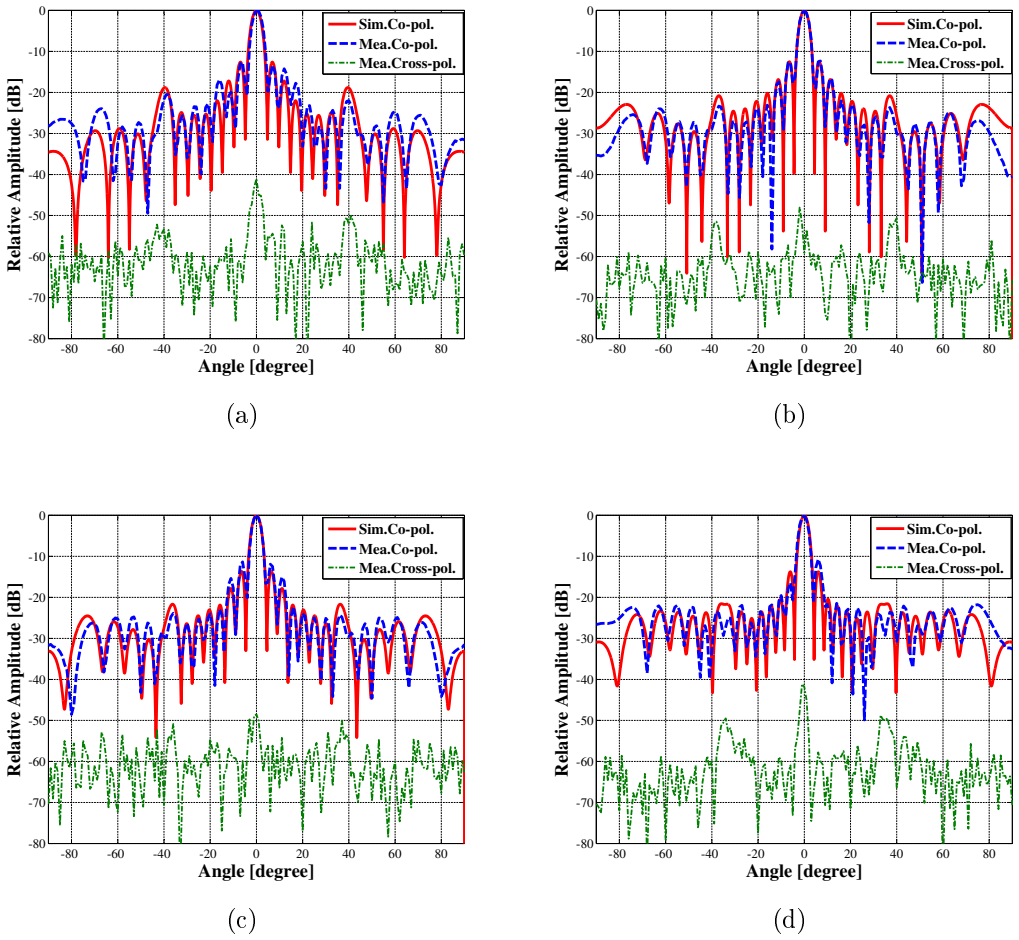

Figure 11: Measured and simulated radiation patterns of the proposed array antenna in E-plane at (a) 57 GHz. (b) 60 GHz. (c) 61 GHz and (d) 66 GHz.

in Fig. 10. The measured S_{11} is a bit higher than the simulation one. However, it is still below -10 dB from 54.5 to 66 GHz (19.2% impedance bandwidth). As discussed in [13], the dispersion diagram of the whole structure is affected by dimensions of metallic pins, the thickness of substrate and the height of air gap. Therefore, any manufacture tolerances of the bed of nails and the height change of air gap will cause a shift for the parallel stopband [16].

The radiation patterns of the proposed antenna were measured in an anechoic chamber in University of Karlsruher. The simulated and measured normalized radiation patterns in both E- and H-planes at four frequencies of 57, 60, 61 and 66 GHz are shown in Figs. 11 and 12. The measured co-polarized radiation patterns show a very good agreement with the simulated results. The simulated and measured radiation patterns are symmetrical, and the first relative side-lobe levels in both E- and H-planes are around -13 dB. The measured grating lobes of the fabricated array

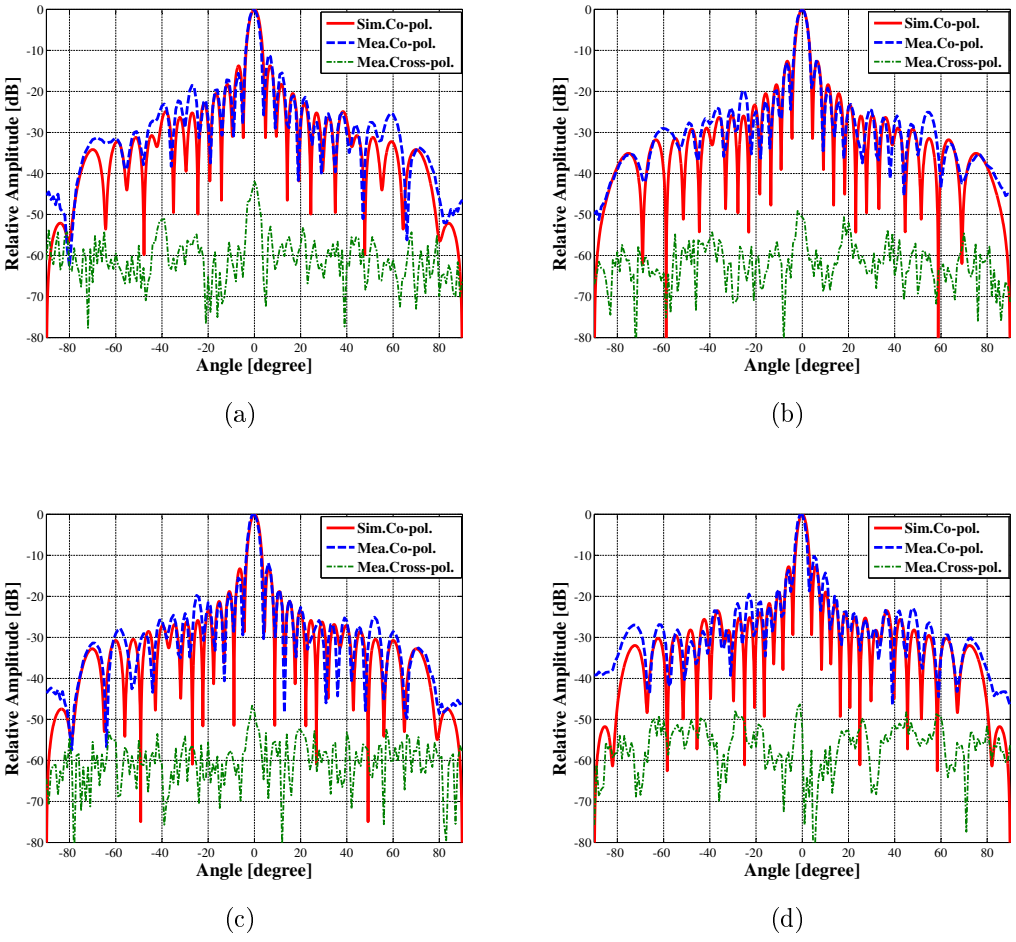

Figure 12: Measured and simulated radiation patterns of the proposed array antenna in H-plane at (a) 57 GHz. (b) 60 GHz. (c) 61 GHz. and (d) 66 GHz.

in both E- and H-planes are below -20 dB over the desired frequency band. The cross-polarized values are below -40 dB at all frequencies.

The simulated and the measured gains of the array antenna are shown in Fig. 13. The pink solid line in Fig. 13 indicates the simulated gain after setting up the modified loss tangent of the substrate (The loss tangent value of RO4003 is manually modified as 0.01 at 60-GHz in CST model). This modification helps us accurately predict the real gain of the antenna. The blue dash line in Fig. 13 shows the measured gain, illustrating above 40% total aperture efficiency over the frequency band

Table 2: COMPARISON BETWEEN THE PROPOSED AND REPORTED 60-GHz PLANAR ANTENNA ARRAYS

Performance	**Ref.**[19]	**Ref.**[4]	**Present Work**
Technology	Plate Laminated	Ridge Gap Waveguide	IMGW
Size [cm]	6.7 × 6.7	7 × 6.4	6.4 × 6.4
Number of Elements	256	256	256
Frequency Band [GHz]	59-64	56-65.7	54.5-64
Bandwidth	8%	16%	17%
Max Gain [dBi]	33	33	30.5
Min Efficiency	80%	70%	40%

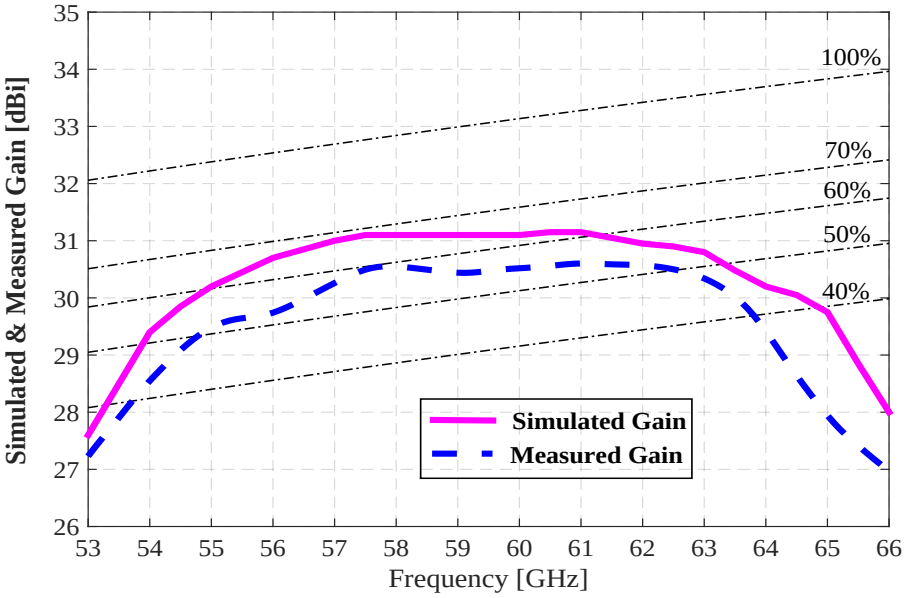

Figure 13: Measured gain and simulated directivity of the present 16 × 16 slot array antenna.

54-64 GHz. What we should notice in Fig. 13 is that the measured gain drops very rapidly starting from 64 GHz, though our design target is 57-66 GHz. The similar phenomena have been also reported in [17] and [18]. The probable explanation for the reduced antenna gain is that the true loss tangent of the substrate may rapidly become larger with the increasing of the frequency and is probably even higher than 0.01 at higher frequency band. The other possible reason for the gain reduction is that the top radiating layer is very thin and therefore any assembly tolerance could cause its deformation which leads to large leakage loss at high frequency.

We summarize structural characteristics and performances of several 60-GHz high-gain antenna arrays, reported in references and compare them with our work in Table II. Compared with the designs in [17] and [18], our work exhibits wide impedance bandwidth, higher aperture efficiency and low cost on fabrication. However, because of the dielectric loss in the substrate of the feeding distribution network, the realized gain of our work is lower than those reported in [4], [6] and [19]. Thereby, there are still some work to do for the further improvements.

5 Conclusion

A high gain and wide bandwidth slot array antenna based on the IMGW technology at 60-GHz has been presented in this paper. The proposed antenna consists of four unconnected layers without any conductive contact between them. The designed prototype is manufactured by EDM technology. The simulated and measured results of the whole antenna structure show very good agreements in radiation patterns in both E- and H-plane. The measured realized gain is higher than 28 dBi over the entire operation bandwidth from 54.5 to 64 GHz, corresponding to efficiency larger than 45%. This work shows that the IMGW technology is an excellent candidate for array antennas in millimeter wave communications.

References

[1] A. Valero-Nogueira, E. Alfonso, J. I. Herranz and P.-S. Kildal, "Experimental demonstration of local quasi-TEM gap modes in singlehard- wall waveguides, " *IEEE Antennas Wireless Propag. Lett.*, vol. 19, no. 9, pp. 536-538, Sep. 2009.

[2] P.-S. Kildal, "Three metamaterial-based gap waveguides between parallel metal plates for mm/submm waves, " in *3rd European Conference on Antennas and Propagation, EuCAP 2009*, pp. 28-32.

[3] H. Raza, J. Yang, P.-S. Kildal and E. Alfonso, "Microstrip-ridge gap waveguide - study of losses, bends, and transition to WR-15, " *IEEE Trans. Microw. Theory Tech.*, vol. 62, no. 9, pp. 1943-1952, 2014.

[4] D. Zarifi, A. Farahbaksh, A. Uz Zaman and P.-S. Kildal, "Design and fabrication of a wideband high-gain 60-GHz corrugated slot antenna array with ridge gap waveguide distribution layer, " *IEEE Trans. Antennas Propag.*, vol. 64, no. 7, pp. 2905-2913, July, 2016.

[5] E. Pucci, E. Rajo-Iglesias, Vazquez-Roy and P.-S. Kildal, "Planar dual-mode horn array with corporate-feed network in inverted microstrip gap waveguide, " *IEEE Trans. Antennas Propag.*, vol. 62, no. 7, pp. 3534-3542, July, 2014.

[6] A. Vosoogh and P.-S. Kildal, "Corporate-Fed planar 60-GHz slot array made of three unconnected metal layers using AMC pin surface for the gap waveguide, "*IEEE Antennas and Wireless Propagation Letters*, December, 2015.

[7] A. Vosoogh and P.-S. Kildal, "High Efficiency 2 $\times$ 2 cavity-backed slot sub-array for 60-GHz planar array antenna based on gap technology, "*2015 International Symposium on Antennas and Propagation (ISAP)*, pp. 1 - 3, Nov. 2015.

[8] A. U. Zaman, P.-S. Kildal and A. A. Kishk, "Narrow-Band Microwave Filter Using High-Q Groove Gap Waveguide Resonators With Manufacturing Flexibility and No Sidewalls, "*IEEE Transactions on Components, Packaging and Manufacturing Technology* , Volume: 2, Issue: 11, Nov. 2012.

[9] A. Vosoogh, A. A. Brazalez and P.-S. Kildal, "A V-Band inverted microstrip gap waveguide end-coupled bandpass filter, "*IEEE Microwave and Wireless Components Letters*, vol. 26, no. 4, April, 2016.

[10] A. U. Zaman, M. Alexanderson, T. Vukusic and P.-S. Kildal, "Gap Waveguide PMC Packaging for Improved Isolation of Circuit Components in High-Frequency Microwave Modules, "*IEEE Transactions on Components, Packaging and Manufacturing Technology*, vol. 4, Issue: 1, Jan. 2014.

[11] E. Rajo-Iglesias, P. S. Kildal, A. U. Zaman, and A. Kishk, "Bed of springs for packaging of microstrip circuits in the microwave frequency range," *IEEE Transaction on Components, Packaging and Manufacturing Technology*, vol. 2, no. 7, July, 2012.

[12] E. Rajo-Iglesias and P.-S. Kildal, "Numerical studies of bandwidth of parallel-plate cut-off realized by a bed of nails, corrugations and mushroom-type electromagnetic bandgap for use in gap waveguides, "*IET Microw.Antennas Propag.*, vol. 5, Iss. 3, pp. 282-289, 2011.

[13] J. L. Liu, A. Uz Zaman and P.-S. Kildal, "Optimizing numerical port for inverted microstrip gap waveguide in full-wave simulators, "*Antennas and Propagation (EUCAP), Proceedings of the 10th European Conference on*, 10-15 April 2016.

[14] J. L. Liu, A. Uz Zaman and P.-S. Kildal, "Design of transition from WR-15 to inverted microstrip gap waveguide, "*2016 Global Symposium on Millimeter Waves (GSMM) Technology and Applications*, 6-8 June 2016.

[15] A. A. Brazález, E. Rajo-Iglesias, J. L. Vázquez-Roy, A. Vosoogh, and P.-S. Kildal, "Design and validation of microstrip gap waveguides and their transitions to rectangular waveguide for millimeter-wave applications, "*IEEE Transactions on Microwave Theory and Techniques*, vol. 63, no. 12, Dec, 2015.

[16] Y. Li and K.-M. Luk, "60-GHz substrate integrated waveguide fed cavity-backed aperture-coupled microstrip patch antenna arrays, " *IEEE Trans. Antennas Propag.*, vol. 61, no. 3, pp. 1075-1085, Jan. 2015.

[17] J. Wu, Y. J. Cheng, and Y. Fan, "A wideband high-gain high-efficiency hybrid integrated plate array antenna for V-Band inter-satellite links, " *IEEE Trans. Antennas Propag.*, vol. 63, no. 4, pp. 1225-1233, Apr. 2015.

[18] Y. Miura, J. Hirokawa, M. Ando, Y. Shibuya and G. Yoshida, "Doublelayer full-corporate-feed hollow-waveguide slot array antenna in the 60 GHz band, " *IEEE Trans. Antennas Propag.*, vol. 59, no. 8, pp. 2844-2851, Aug. 2011.